Optics Letters

Self-stabilization of an optical frequency comb using a short-path-length interferometer

James P. Cahill,[1,*] Weimin Zhou,[1] and Curtis R. Menyuk[2]

[1]U.S. Army Research Laboratory, 2800 Powder Mill Road, Adelphi, Maryland 20783, USA
[2]Department of Computer Science and Electrical Engineering, University of Maryland: Baltimore County, 1000 Hilltop Circle, Baltimore, Maryland 21250, USA
*Corresponding author: james.p.cahill15.civ@mail.mil

Received 20 February 2017; revised 30 March 2017; accepted 31 March 2017; posted 31 March 2017 (Doc. ID 286730); published 20 April 2017

We stabilized the repetition rate of an optical frequency comb using a self-referenced phase-locked loop. The phase-locked loop generated its error signal with a fiber-optic delay-line interferometer that had a path-length difference of 8 m. We used the stabilized repetition rate to generate a 10 GHz signal with a single-sideband phase noise that was limited by environmental noise to −120 dBc/Hz at an offset frequency of 1 kHz. Modeling results indicate that thermoconductive noise sets a fundamental phase noise limit for an 8 m interferometer of −152 dBc/Hz at a 1 kHz offset frequency. The short length of the interferometer indicates that it could be realized as a photonic integrated circuit, which may lead to a chip-scale stabilized optical frequency comb with an ultralow-phase-noise repetition rate.

OCIS codes: (140.3425) Laser stabilization; (060.5625) Radio frequency photonics; (140.7090) Ultrafast lasers; (140.4050) Mode-locked lasers.

https://doi.org/10.1364/OL.42.001680

A multitude of systems, including radar, remote sensing, very-long-baseline interferometry, and quantum information systems, require microwave frequency sources that generate signals at 10 GHz and higher with ultralow phase noise. These systems will benefit from ultralow-phase-noise frequency sources that are compact, inexpensive, and scalable to mass production. Optical cavities, such as ultralow expansion glass Fabry–Perot cavities or crystalline whispering gallery mode resonators, have been used to generate optical frequencies that are exceedingly stable over short time scales [1,2], reaching Allan deviations, for example, of approximately 1×10^{-16} at 1 s. When these optical frequencies are coherently divided, they produce ultralow-phase-noise microwave signals. Optical frequency combs (OFCs) have emerged as an elegant way to perform this coherent frequency division [3]. This technique has led to the generation of signals at numerous frequencies from 5 MHz to 10 GHz with record-breaking low-phase-noise levels [4,5]. However, the Fabry–Perot cavities and whispering gallery mode resonators that achieve the lowest phase noise typically require extensive environmental isolation, are hand-manufactured, and cannot be monolithically integrated. These factors result in a frequency source that is necessarily large and expensive.

An alternative approach is to use an optical delay-line interferometer, such as an asymmetric Mach–Zehnder interferometer (AMZI) or Michelson interferometer, to measure the phase noise of the OFC's repetition rate and cancel it in real time using a phase-locked loop (PLL). This technique has been used to narrow the linewidth of continuous-wave lasers to less than 1 Hz [6–9] and ultimately achieved a frequency stability of 7×10^{-15} at 1 s using a fiber-optic interferometer with a path-length difference of 500 m [9]. The technique has also been applied to an OFC in order to generate a 10 GHz signal with a phase noise of −130 dBc/Hz at 1 kHz offset frequency using a fiber-optic interferometer with a 2 km path-length difference [10]. Because of their simple architecture, delay-line interferometers with short-path-length imbalances can be monolithically integrated using a straightforward and scalable manufacturing process. However, the delay lengths used in the existing literature are too long to be achieved on an integrated platform.

In the work reported in this Letter, we investigated the phase noise limits of the repetition rate of an OFC that was stabilized using a short-path-length AMZI. We used an AMZI with an 8 m path imbalance to generate a 10 GHz signal with a phase noise of −120 dBc/Hz at a 1 kHz offset frequency. In addition, we developed a model that accounts for environmental, thermoconductive, RF-component, and shot noise. We found that the thermoconductive and RF noise contributions rise as the delay length is decreased, while the environmental and shot noise contributions remain constant. Thus, when using an AMZI-stabilized OFC to generate a low-phase-noise microwave, the phase noise requirements will set a minimum length for the AMZI path imbalance. We compared the model and experimental results and found that the phase noise of the 10 GHz signal was dominated by environmental noise at offset frequencies below 10 kHz and by shot noise at offset frequencies above 10 kHz. Both of these noise sources could be mitigated in future work. The model further indicated that if the environmental and shot noise contributions were mitigated, the ultimate phase noise limitation when using an 8 m long

delay would be the thermoconductive noise. We estimated this limitation to be −152 dBc/Hz at a 1 kHz offset. A path difference of less than 10 m indicates that this stabilization scheme could be realized as a photonic integrated circuit. Low-loss optical delay lines as long as 29 m have been demonstrated using monolithic integrated Si_3N_4 waveguides [11]. In combination with the development of integrated Kerr-comb OFCs [12,13], this technology may provide a small-scale, fully integrated method to generate ultralow-phase-noise microwaves.

The output of an OFC has frequency components at $\omega_N = N\omega_r + \omega_{CEO}$, where N is an integer that is typically of the order of 10^5, ω_r is the OFC's repetition rate, and ω_{CEO} is the OFC's carrier-envelope offset frequency (CEO frequency). Figure 1 shows the experimental setup that we used to stabilize the OFC and generate the 10 GHz signal. The output of a commercially available OFC (Menlo Systems FC-1500, center wavelength of 1550 nm, repetition rate of 250 MHz) was split into two different circuits. The circuit in the yellow box, labeled "10 GHz Out," generated the 10 GHz signal. The light from the OFC illuminated a fast P-I-N photodiode (PD) and excited a photocurrent with frequency components at $\omega_m = m\omega_r$, where m is an integer. A bandpass filter (BPF) selected the component closest to 10 GHz. The circuit in the blue box, labeled "Rep. Rate Stabilization," stabilized the repetition rate of the OFC by applying negative feedback of the phase noise of ω_N to the repetition rate. The phase noise of ω_N is a function of both the repetition rate noise and the CEO-frequency noise. Because the contribution of the CEO-frequency noise to the phase noise of ω_N is comparable to the contribution of the repetition rate noise, the CEO noise contribution must be removed in order for the stabilization scheme to be effective. To accomplish this removal, we sent the light from the OFC into an acousto-optic frequency shifter (AOFS1). A commercially available $1f-2f$ interferometer directly measured the CEO frequency of the OFC. The CEO frequency was fed into the RF input of AOFS1, so that the light that emerged from AOFS1 had frequency components at $\omega_N = N\omega_r$, and the frequency shift and phase noise due to the CEO frequency were eliminated from the output of AOFS1 [14].

The light at the output of AOFS1 was then split by a 50% power coupler. One portion of the light passed through another acousto-optic frequency shifter (AOFS2), which shifted the frequency by 60 MHz in order to allow heterodyne detection. The other portion of the light propagated through a 40 ns (8 m) hybrid free-space/fiber-optic delay, which could be tuned over a range of 3 ns with a precision of approximately 0.1 ps.

The frequency-shifted and time-delayed components of the light were recombined using a 2 × 2 50% power coupler, thereby creating an AMZI with a path-length difference of 8 m. The output beams of the AMZI illuminated a pair of balanced photodiodes (BPDs), which generated a signal at the heterodyne frequency of 60 MHz. The tunable delay was adjusted to ensure that pulses that traveled different paths in the AMZI overlapped on the photodiodes. The tunable delay would not be required in a chip-based system, where the path-length imbalance could be precisely controlled during fabrication. The 60 MHz output of the balanced photodiodes had the phase noise of the optical signal, as filtered by the transfer function of the AMZI. We used an RF mixer as a phase detector, where the reference was the same signal that drove AOFS2. The output signal of the phase detector passed through a proportional-integral (PI-)loop filter and was fed back to an electro-optic phase modulator (EOM) within the cavity of the OFC in order to stabilize the repetition rate.

In order to identify the dominant noise contributions to the phase of the repetition rate, $\phi_r(\omega)$, we developed Fourier-domain models that describe each circuit, as depicted in Fig. 2. We modeled the 10 GHz generation circuit as a frequency multiplier since the signal that emerges from the 10 GHz output is the mth harmonic of the repetition rate.

We modeled the stabilization circuit as a PLL, following the approach of [15]. We considered the effects of three generalized noise sources, which are highlighted by the red boxes. We assumed that the cancellation of both the CEO frequency and heterodyne frequency was complete, so we neglected their noise in the model. The first generalized noise source was the instantaneous phase noise of the repetition rate, $\phi_0(\omega)$. This noise is what the PLL operates to suppress. In addition, all of the RF components, including the mixer and loop filter, introduce noise into the in-loop voltage signal. We represented these noise contributions with an aggregate RF noise term, $v_{RF}(\omega)$, which we added to the in-loop voltage signal following the phase detector. The final noise source that we considered was the additive optical phase noise of the delay within the AMZI, $\phi_{opt}(\omega)$.

At the output of the OFC, we considered the Nth harmonic of the repetition rate, which has a phase of $N \times \phi_r(\omega)$. This signal is split in two paths. The signal in one path passes through AOFS2, which we have neglected in this analysis,

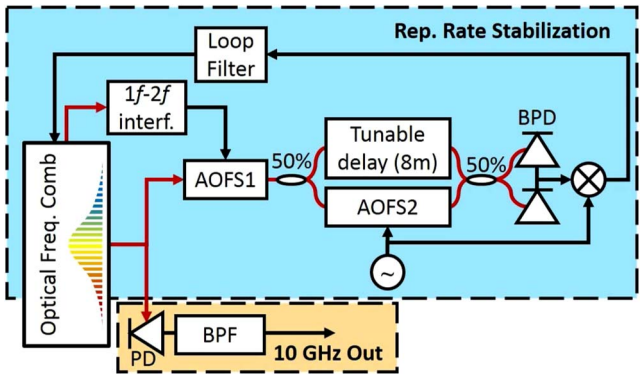

Fig. 1. Diagram of the circuit used to stabilize the repetition rate of the frequency comb (blue box) and the circuit used to generate the 10 GHz signal (yellow box).

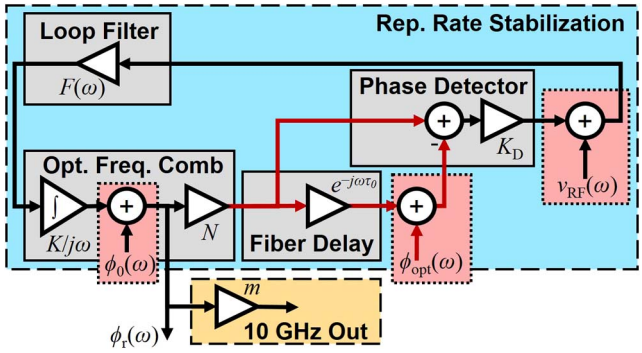

Fig. 2. Illustration of the Fourier-domain model of the circuits used to stabilize the optical frequency comb and generate the 10 GHz signal. The red-shaded boxes indicate additive noise sources.

and subsequently enters one arm of a 50% coupler. The signal in the other path passes through the tunable fiber-optic delay, which imparts a group delay of τ_0 and an additive noise term, ϕ_{opt}. The signal subsequently enters the other arm of the 50% coupler. The 50% coupler, BPD, and RF mixer operate together as a phase detector whose output is equal to the difference of the phases of the signals at the input of the coupler multiplied by the phase-to-voltage ratio of the RF mixer, K_{D}. The voltage signal that emerges from the phase detector, $v_{\text{PD}}(\omega)$, is given by

$$v_{\text{PD}}(\omega) = NK_{\text{D}}[\phi_{\text{r}}(\omega) - e^{-j\omega\tau_0}\phi_{\text{r}}(\omega)] + K_{\text{D}}\phi_{\text{opt}}(\omega). \quad (1)$$

The signal out of the phase detector is added to the voltage noise term $v_{\text{RF}}(\omega)$ and passes through the loop filter. The loop filter imparts frequency-dependent gain to the voltage signal with a transfer function of $F(\omega)$, and the output of the loop filter is fed back into the input of the intracavity EOM. The EOM alters the OFC's repetition rate in proportion to the voltage signal at the output of the loop filter, with a voltage-to-frequency coefficient of K. Hence, the EOM acts as an integrator with respect to the phase of the repetition rate, with a transfer function of $K/j\omega$. Therefore, we can write a recursive equation for $\phi_{\text{r}}(\omega)$ as

$$\phi_{\text{r}}(\omega) = \frac{F(\omega)K}{j\omega}[v_{\text{PD}}(\omega) + v_{\text{RF}}(\omega)] + \phi_0(\omega). \quad (2)$$

We can use Eq. (1) to solve Eq. (2) explicitly for $\phi_{\text{r}}(\omega)$ as

$$\phi_{\text{r}}(\omega) = H(\omega) \times \left[\frac{KK_{\text{D}}F(\omega)}{j\omega}\phi_{\text{opt}}(\omega) + \frac{KF(\omega)}{j\omega}v_{\text{RF}}(\omega) + \phi_0(\omega)\right], \quad (3)$$

where we have defined the loop transfer function

$$H(\omega) \equiv \frac{j\omega}{j\omega - NKK_{\text{D}}F(\omega)[1 - \exp(-j\omega\tau_0)]}. \quad (4)$$

We are interested in the power spectral density (PSD) of the phase, which can be found by taking the square magnitude of Eq. (3). For offset frequencies for which $\omega\tau_0 \ll 1$, we make the approximation

$$|H(\omega)|^2 \approx \left|\frac{1}{N\tau_0 KK_{\text{D}}F(\omega)}\right|^2. \quad (5)$$

Using Eqs. (3) and (5), the PSD of the repetition rate phase noise, $S_{\phi,\text{r}}(\omega)$, is

$$S_{\phi,\text{r}}(\omega) = \left(\frac{1}{N\tau_0\omega}\right)^2\left[S_{\phi,\text{opt}}(\omega) + \frac{1}{K_{\text{D}}^2}S_{v,\text{RF}}(\omega)\right], \quad (6)$$

where $S_{\phi,\text{opt}}(\omega)$ is the PSD of the additive optical phase noise, and $S_{v,\text{RF}}(\omega)$ is the PSD of the RF components' voltage noise term, $v_{\text{RF}}(\omega)$. We have assumed that the loop filter has an arbitrarily large gain for the offset frequencies of interest, so that the contribution of the instantaneous phase noise can be neglected.

We would like to use Eq. (6) to elucidate the dependence of $S_{\phi,\text{r}}$ on the delay length. However, the additive optical phase noise depends implicitly on both N and τ_0. Consequently, we must consider contributions to the optical phase noise from both environmentally induced fluctuations and spontaneous fluctuations of the group delay through the AMZI. For most offset frequencies of interest, the spontaneous delay fluctuations are well described by spontaneous fluctuations of the temperature, also known as the thermoconductive noise [16,17].

Environmental fluctuations impinge upon the tunable fiber-optic delay, so that the instantaneous group delay, τ, is given by $\tau = \tau_0 + \delta\tau$, where τ_0 is the average group delay and $\delta\tau$ represents the environmentally induced fluctuations of the group delay. We assumed that $\delta\tau$ is proportional to the average group delay. Hence, $\delta\tau = \tau_0\delta x_{\text{env}}$, where x_{env} represents the fractional fluctuations of the group delay that result from environmental fluctuations. The group-delay fluctuations lead to an additive phase noise contribution, $\phi_{\text{env}}(\omega)$, equal to

$$S_{\phi,\text{env}}(\omega) = (N\omega_{\text{r}}\tau_0)^2 S_{x,\text{env}}(\omega). \quad (7)$$

Hence, we expect the additive phase noise due to environmental fluctuations to be proportional to τ_0^2.

The spontaneous temperature fluctuations cause optical phase noise by the same processes as an external temperature fluctuation does; however, the PSD of the spontaneous temperature fluctuations is inversely proportional to the delay length [16,17]. Hence, in contrast to the environmental noise, we expect the thermoconductive noise to be proportional to τ_0. We have

$$S_{\phi,\text{TC}}(\omega) = (N\omega_{\text{r}})^2\tau_0 S_{\text{TC}}(\omega), \quad (8)$$

where $S_{\text{TC}}(\omega)$ represents the frequency dependence of the thermoconductive noise, which can be found using [17].

We combine Eqs. (6)–(8) to obtain a formula for the noise sources that explicitly includes their dependencies on the delay length. We have

$$S_{\phi,\text{r}}(\omega) = \left(\frac{1}{\omega}\right)^2\left[\omega_{\text{r}}^2 S_{x,\text{env}}(\omega) + \frac{\omega_{\text{r}}^2}{\tau_0}S_{\text{TC}}(\omega) + \left(\frac{1}{NK_{\text{D}}\tau_0}\right)^2 S_{v,\text{RF}}(\omega)\right]. \quad (9)$$

The first term of Eq. (9) shows that the environmental noise contribution to $S_{\phi,\text{r}}(\omega)$ does not depend on the delay length τ_0. By contrast, the thermoconductive noise is inversely proportional to τ_0, and the noise contribution of the RF components is inversely proportional to τ_0^2, so that using a longer path-length difference in the AMZI would reduce the contribution of these two noise sources. Hence, the length of the delay should be determined, so that the RF and thermoconductive noise contributions are below the phase noise requirement.

Equation (9) also elucidates the main advantage of using an OFC in the PLL. The PLL error signal is generated from the phase noise of the optical frequency, $N\omega_{\text{r}}$, so that the noise contribution to $S_{\phi,\text{r}}(\omega)$ of the RF components is effectively divided by the large factor N^2. In addition, the environmental, thermoconductive, and RF noise contributions are inversely proportional to the factor ω^2, which indicates that the noise contribution will be amplified as the offset frequency decreases, regardless of which noise source is dominant. Since the frequency stability over long time scales is heavily weighted by the phase noise at low offset frequencies, the PLL is less effective at stabilizing the repetition rate over long time scales.

To characterize the performance of the stabilization scheme, we measured the phase noise of the signal emerging from the 10 GHz generation circuit. The results are shown as the black line in Fig. 3. For offset frequencies above 10 kHz, the phase noise of the OFC-generated signal was approximately −144 dBc/Hz. For offset frequencies below 10 kHz, its phase noise rose sharply, reaching approximately −120 dBc/Hz at 1 kHz and approaching −40 dBc/Hz at 10 Hz. The phase noise level at an offset of 10 Hz indicates that the

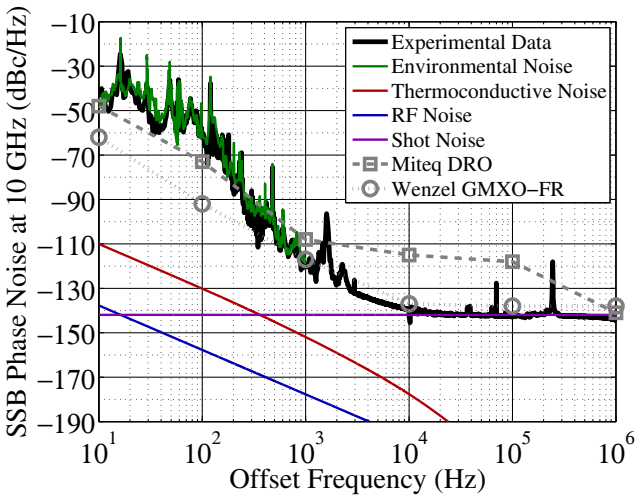

Fig. 3. Phase noise of the 10 GHz signal generated by the OFC (black). The phase noise of two commercially available 10 GHz sources are plotted for comparison (squares and circles). Also plotted are the noise contributions of several mechanisms (colored lines).

OFC-generated signal will not have good long-term frequency stability. The peak that occurs at approximately 250 kHz was due to a resonance in the PLL. Its amplitude may be reduced with a more careful design of the loop transfer function.

Figure 3 also shows the phase noise of two commercially available low-phase-noise 10 GHz sources: a dielectric resonant oscillator (DRO) distributed by Miteq (boxes) and a multiplied-quartz oscillator (GMXO-FR) designed by Wenzel (circles) [18,19]. For offset frequencies above 1 kHz, the OFC-generated signal has significantly lower phase noise than the DRO but only marginally lower phase noise than the GMXO-FR.

We evaluated Eq. (3) in order to investigate both the current and ultimate limits of this technique and plotted the results in Fig. 3. In addition to the noise sources in Eq. (3), we also accounted for the shot noise in the PD in the 10 GHz generation circuit. We directly measured the environmentally induced noise by sending the light from a low-phase-noise continuous-wave laser (NKT Photonics Koheras Adjustik) through the AMZI. The measurement was restricted to offset frequencies of 10 Hz–1 kHz because the laser phase noise dominated the measurement at offset frequencies above 1 kHz.

The noise contributions from environmental (green) and shot noise (purple) match the experimentally measured phase noise from offset frequencies of 10 Hz–1 kHz and 10 kHz–1 MHz, respectively. Hence, our system was limited by environmental noise and shot noise. In this work, the impact of the environmental fluctuations was relatively high because acoustics and temperature fluctuations were uncontrolled. The AMZI was placed in open air on a standard air-damped optical table in a laboratory setting with no external enclosure or additional environmental isolation. With careful packaging, we expect that the environmentally induced noise could be reduced. The shot noise level could be reduced by increasing the average optical power of the OFC or by increasing the proportion of the total power in the 10 GHz harmonic. The power in the 10 GHz harmonic could be increased by using an OFC with a higher repetition rate or by using a repetition rate multiplier [20].

The ultimate limitations of this stabilization technique are determined by the thermoconductive and RF noise contributions, which are shown in Fig. 3 by the red and blue lines, respectively. Both of these noise sources are length dependent; we modeled their expected contributions for the case of an 8 m fiber-optic delay. We estimated the RF noise contribution using a mixer phase-to-voltage gain, K_D, of 0.46 V/rad. We attributed the voltage noise, $S_{v,RF}$, to the thermal noise across the output impedance (500Ω) of the mixer, which resulted in a voltage spectral density of −171 dBV/Hz. The corresponding contribution to the 10 GHz phase noise is −178 dBc/Hz at 1 kHz offset frequency. The estimated thermoconductive contribution to the 10 GHz phase noise is −152 dBc/Hz at 1 kHz offset frequency. Hence, for a delay of 8 m, the thermoconductive noise sets the expected phase noise limitation.

In summary, we used an AMZI with an 8 m path-length difference to stabilize the repetition rate of an OFC. We used the stabilized repetition rate to generate a 10 GHz signal with a phase noise of −120 dBc/Hz at a 1 kHz offset frequency. We demonstrated that the phase noise in our experiments was limited by environmental noise at offset frequencies below 10 kHz and by shot noise at offset frequencies above 10 kHz. We described a model whose results indicate that, if the environmental and shot noise are mitigated, an OFC stabilized by an 8 m delay could generate a 10 GHz signal with a phase noise of −152 dBc/Hz at 1 kHz offset. The use of a path-length difference of less than 10 m points the way toward realizing this technique as a photonic integrated circuit.

REFERENCES

1. S. Häfner, S. Falke, C. Grebing, S. Vogt, T. Legero, M. Merimaa, C. Lisdat, and U. Sterr, Opt. Lett. **40**, 2112 (2015).
2. J. Alnis, A. Schliesser, C. Y. Wang, J. Hofer, T. J. Kippenberg, and T. W. Hänsch, Phys. Rev. A **84**, 011804 (2011).
3. D. J. Jones, S. A. Diddams, J. A. Ranka, A. Stentz, R. S. Windeler, J. L. Hall, and S. T. Cundiff, Science **288**, 635 (2000).
4. T. M. Fortier, F. Quinlan, A. Hati, C. Nelson, J. A. Taylor, Y. Fu, J. Campbell, and S. A. Diddams, Opt. Lett. **38**, 1712 (2013).
5. A. Hati, C. W. Nelson, C. Barnes, D. Lirette, T. Fortier, F. Quinlan, J. A. DeSalvo, A. Ludlow, S. A. Diddams, and D. A. Howe, IEEE Trans. Ultrason. Ferroelectr. Freq. Control **60**, 1796 (2013).
6. Y. T. Chen, Appl. Opt. **28**, 2017 (1989).
7. B. S. Sheard, M. B. Gray, and D. E. McClelland, Appl. Opt. **45**, 8491 (2006).
8. F. Kéfélian, H. Jiang, P. Lemonde, and G. Santarelli, Opt. Lett. **34**, 914 (2009).
9. J. Dong, Y. Hu, J. Huang, M. Ye, Q. Qu, T. Li, and L. Liu, Appl. Opt. **54**, 1152 (2015).
10. K. Jung and J. Kim, Sci. Rep. **5**, 16250 (2015).
11. H. Lee, T. Chen, J. Li, O. Painter, and K. J. Vahala, Nat. Commun. **3**, 867 (2012).
12. D. J. Moss, R. Morandotti, A. L. Gaeta, and M. Lipson, Nat. Photonics **7**, 597 (2013).
13. V. Brasch, M. Geiselmann, T. Herr, G. Lihachev, M. H. P. Pfeiffer, M. L. Gorodetsky, and T. J. Kippenberg, Science **351**, 357 (2016).
14. S. Koke, C. Grebing, H. Frei, A. Anderson, A. Assion, and G. Steinmeyer, Nat. Photonics **4**, 462 (2010).
15. F. M. Gardner, *Phaselock Techniques*, 3rd ed. (Wiley, 2005).
16. K. H. Wanser, Electron. Lett. **28**, 53 (1992).
17. L. Duan, Phys. Rev. A **86**, 023817 (2012).
18. L3 Narda-MITEQ, "Frequency Generation Products," http://www.miteq.com/docs/MITEQ_FreqSource_c38.pdf.
19. Wenzel Associates, Inc., "GMXO-FR," http://www.wenzel.com/model/gmxofr/.
20. A. Haboucha, W. Zhang, T. Li, M. Lours, A. N. Luiten, Y. LeCoq, and G. Santarelli, Opt. Lett. **36**, 3654 (2011).